Autoinhibition of Mint1 adaptor protein regulates amyloid precursor protein binding and processing

Maria F. Matos[a,1], Yibin Xu[b,1], Irina Dulubova[c], Zbyszek Otwinowski[b], John M. Richardson[d,2], Diana R. Tomchick[b], Josep Rizo[b], and Angela Ho[a,3]

[a]Department of Biology, Boston University, 5 Cummington Street, Boston, MA 02215; [b]Departments of Biochemistry and [d]Physiology, University of Texas Southwestern Medical Center, 5323 Harry Hines Boulevard, Dallas, TX 75390; and [c]Reata Pharmaceuticals, Inc., 2801 Gateway Drive, Suite 150, Irving, TX 75063

Edited* by Thomas C. Südhof, Stanford University School of Medicine, Palo Alto, CA, and approved January 13, 2012 (received for review November 18, 2011)

Mint adaptor proteins bind to the amyloid precursor protein (APP) and regulate APP processing associated with Alzheimer's disease; however, the molecular mechanisms underlying Mint regulation in APP binding and processing remain unclear. Biochemical, biophysical, and cellular experiments now show that the Mint1 phosphotyrosine binding (PTB) domain that binds to APP is intramolecularly inhibited by the adjacent C-terminal linker region. The crystal structure of a C-terminally extended Mint1 PTB fragment reveals that the linker region forms a short α-helix that folds back onto the PTB domain and sterically hinders APP binding. This intramolecular interaction is disrupted by mutation of Tyr633 within the Mint1 autoinhibitory helix leading to enhanced APP binding and β-amyloid production. Our findings suggest that an autoinhibitory mechanism in Mint1 is important for regulating APP processing and may provide novel therapies for Alzheimer's disease.

Mints [also known as X11s or amyloid precursor protein (APP) binding, family A] are a family of adaptor proteins encoded by three genes: neuron-specific Mint1 and Mint2, and the ubiquitously expressed Mint3 (1, 2). Mints consist of a divergent N-terminal region and conserved C-terminal sequences composed of a phosphotyrosine binding (PTB) domain and two tandem PDZ (postsynaptic density-95/discs large/zona occludens-1) domains. The PTB domain of all Mints interacts directly with a conserved YENPTY cytoplasmic motif of the APP that is essential for regulating APP trafficking and processing (3–6). APP is a type I transmembrane protein that is sequentially cleaved by site-specific proteases (7–10). Abnormal processing of APP generates Aβ peptides leading to the accumulation of extracellular plaques that are characteristic of Alzheimer's disease (AD). β-Secretase is the first amyloidogenic cleavage, generating a soluble APP ectodomain (sAPPβ) and a C-terminal fragment (CTFβ). CTFβ is subsequently cleaved by γ-secretase (a protein complex of anterior pharyx defective 1, nicastrin, presenilin, and presenilin enhancer 2) to release the small peptides Aβ40 and Aβ42, the latter having an increased propensity to form amyloid aggregates found in the brains of AD patients (11–14). Alternatively, APP is sequentially cleaved by α-secretase within the Aβ region then γ-secretase, which initiates the nonamyloidogenic or nontoxic pathway (9, 10).

Considerable evidence indicates that the APP-Mint interaction is biologically significant because loss of each individual Mint protein delays age-dependent production of amyloid plaques in transgenic AD mouse models (15). Past studies have indicated that the N- and C-terminal regions of Mints play an important role in regulating APP binding and cleavage events based on deletion analysis of Mints in a heterologous expression system (6, 16). The Mint N terminus was shown to promote APP binding and Aβ production, whereas the C-terminal region disrupted PTB-mediated binding to APP and decreased Aβ peptides (6, 16). However, the structural basis and the physiological regulation of APP processing by Mints in neurons have not been elucidated. Using a combination of biochemical, biophysical, and cell biological techniques, we now show that binding of APP to the Mint1 PTB domain is regulated by the conformational state of Mint1. The three-dimensional structure of a Mint1 fragment reveals that the PTB domain is autoinhibited by a helical motif that lays immediately C-terminal to the PTB domain, and directly occludes the APP interaction site. In addition, we show that Tyr633 of Mint1 is key for the hydrophobic interactions that underlie inhibition of APP binding and that mutation of this residue enhances APP binding and processing. These results show that Mint1 undergoes a conformational switch between a "closed" state that does not bind APP and an "open" state involved in APP binding and processing events.

Results

The C-Terminal Region of Mint1 Inhibits PTB-Mediated Binding to APP. To gain a better understanding of how the C-terminal portion of Mint1 affects PTB-mediated APP binding and to determine whether this is a common feature of Mint proteins, we produced T7-tagged recombinant rat Mint1 fusion proteins that contained the PTB domain and C-terminal extensions including 13 residues of the PTB-PDZ1 linker region ($Mint1^{453–635}$), 21 residues of the linker region ($Mint1^{453–643}$), the first PDZ domain ($Mint1^{453–749}$), both PDZ domains ($Mint1^{453–824}$), and both PDZ domains with the C-terminal tail ($Mint1^{453–839}$). All recombinant proteins were immobilized on T7 antibody-coupled agarose and used in pull-down experiments to test their ability to bind APP from HEK293T cells overexpressing APP or rat brain lysate (Fig. 1 *A* and *B*). The Mint1 PTB domain pulled down APP from brain lysate, consistent with previous studies (3), and the other APP family members APP-like protein 1 and 2 (APLP1 and APLP2) (Fig. 1*B*). However, C-terminal extension of the PTB domain dramatically reduced its binding to APP, APLP1, and APLP2. Extension of the linker region downstream of the Mint1 PTB domain by only eight amino acids (from $Mint1^{453–635}$ to $Mint1^{453–643}$) virtually eliminated all APP, APLP1, and APLP2 binding from rat brain lysate (Fig. 1*B* and Fig. S1), and greatly decreased APP binding from transfected cells (Fig. 1*A*). T7 antibody agarose alone and the Mint1 N-terminal Munc18-1 interacting domain ($Mint1^{220–321}$) served as negative controls and did not bind APP. We observed similar inhibition of PTB-mediated binding to APP in the presence of the N-terminal sequences preceding the PTB domain, and we detected mini-

Author contributions: M.F.M., Y.X., I.D., J.R., and A.H. designed research; M.F.M., Y.X., I.D., and J.M.R. performed research; M.F.M., Y.X., Z.O., D.R.T., J.R., and A.H. analyzed data; and J.R. and A.H. wrote the paper.

The authors declare no conflict of interest.

*This Direct Submission article had a prearranged editor.

Data deposition: The atomic coordinates and structure factors have been deposited in the Protein Data Bank, www.pdb.org (PDB ID code 4DBB; Research Collaboratory for Structural Bioinformatics ID RCSB070115).

[1]M.F.M. and Y.X. contributed equally to this work.

[2]Present address: Department of Chemistry, Austin College, 900 North Grand Avenue, Sherman, TX 75090.

[3]To whom correspondence should be addressed. E-mail: aho1@bu.edu.

This article contains supporting information online at www.pnas.org/lookup/suppl/doi:10.1073/pnas.1119075109/-/DCSupplemental.

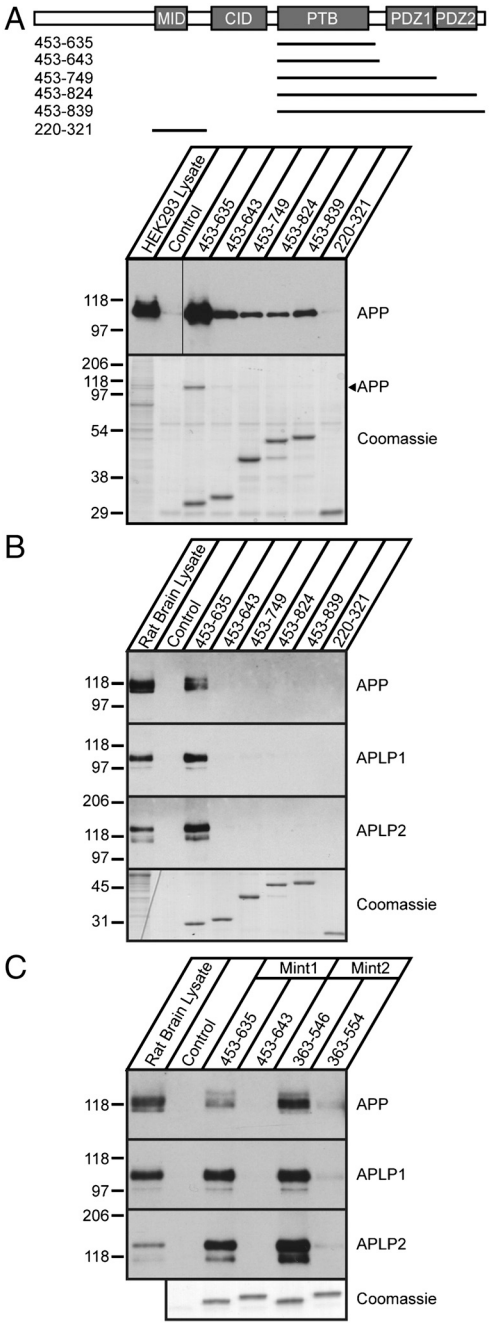

Fig. 1. C-terminal sequences of neuronal Mint proteins inhibit PTB-mediated binding to APP. (*A*) Schematic of T7-tagged rat Mint1 recombinant proteins used. Numbers on the left indicate amino acid positions. The Munc18-1 interacting domain (MID; residues 220–321) and T7 antibody agarose alone (control) were used as negative controls. Western blot analysis of APP from transiently transfected HEK293T cells bound to different Mint1 recombinant proteins. CID, CASK interacting domain. (*B*) Western blot analysis of APP and APLPs from rat brain lysate bound to the different Mint1 recombinant proteins. (*C*) Western blot analysis of APP from rat brain lysate bound to Mint1 and Mint2 recombinant proteins. (*A–C*, *Bottom*) Coomassie stained gels of T7-tagged Mint proteins.

mal APP binding with the full-length Mint1 protein, suggesting that the N terminus of Mint1 does not alleviate the inhibitory effect of the C-terminal extensions on APP binding (Fig. S2).

Given that the C terminus of Mint1 and Mint2 are highly conserved and loss of either Mint1 or Mint2 leads to a reduction in Aβ production (15), we next examined whether the corresponding Mint2 linker sequence C-terminal to its PTB domain also interferes with APP binding from brain and APP overexpressing HEK293T cells. To this end, we generated Mint2 fragments containing the PTB domain with ($Mint2^{363–554}$) and without the putative inhibitory sequence ($Mint2^{363–546}$) and performed pull-down assays (Fig. 1*C* and Fig. S3). The PTB domains of both Mint1 and Mint2 bound APP from brain, with APP binding relatively stronger for Mint2 than Mint1. Similar to Mint1, the linker sequences C-terminal to the Mint2 PTB domain reduced APP binding. We also found that Mint2 can bind to all members of the APP family of proteins, consistent with previous observations (6), and the eight residue addition to the C-terminal linker of the Mint2 PTB domain also disrupted APLP1 and APLP2 binding. Taken together, these results show that the C-terminal regions of Mints 1 and 2 are critical for inhibiting PTB-mediated binding to the APP family of proteins in brain. Moreover, the enhancement of APP binding to the PTB domain by removal of C-terminal flanking sequences suggests the presence of autoinhibitory regulatory elements in full-length Mint proteins, and strongly implicates the C-terminal region of Mints 1 and 2 in the inhibitory function.

Mechanism of Inhibition by Mint1 C-Terminal Sequences. To investigate the structural basis for the inhibition of APP binding by Mint1 C-terminal sequences, we first employed NMR spectroscopy. We expressed and purified ^{15}N-labeled fragments corresponding to the Mint1 PTB domain ($Mint1^{453–635}$) and to the PTB domain plus the minimal linker region necessary for inhibiting PTB-mediated binding to APP ($Mint1^{453–643}$), and acquired their ^{1}H-^{15}N heteronuclear single quantum correlation (HSQC) spectra. The ^{1}H-^{15}N HSQC spectrum of $Mint1^{453–635}$ exhibited unusual cross-peak broadening that is indicative of protein instability or aggregation (Fig. 2*A*, black contours). However, the ^{1}H-^{15}N HSQC spectrum of $Mint1^{453–635}$ in the presence of the 15 amino acid APP C-terminal peptide GQNGYENPTYKFFEQ (red contours) showed well-dispersed cross-peaks and clear shifts in multiple cross-peaks (Fig. 2*A*), demonstrating that the APP peptide binds to the PTB domain and stabilizes it or hinders its aggregation. Interestingly, the ^{1}H-^{15}N HSQC spectrum of $Mint1^{453–643}$ in the absence of APP peptide (Fig. 2*B*, blue contours) showed well-dispersed cross-peaks and much less broadening than the spectrum of $Mint1^{453–635}$ alone (black contours). These observations show that the additional C-terminal linker residues stabilize the PTB domain or impede its aggregation, similar to the effect of APP-peptide binding. This effect can be attributed to intramolecular interactions between the additional C-terminal linker residues and the PTB domain, which may compete with the APP peptide for binding to the PTB domain.

The inhibitory interaction between $Mint1^{453–643}$ and APP was further investigated by isothermal titration calorimetry (ITC). ITC titrations showed that $Mint1^{453–635}$ has a stronger affinity for the APP C-terminal peptide ($K_d = 0.78$ μM) than $Mint1^{453–643}$ (estimated $K_d = 25.5$ μM), consistent with the pull-down and NMR data (Fig. S4). Together, these results show that the PTB domain retains tight binding to APP; however, the residues C-terminal to the PTB domain form an intramolecular interaction with the PTB domain that impairs APP binding.

Crystal Structure of the Mint1 PTB Domain and Mechanism of Autoinhibition. The crystal structure of the Mint1 PTB domain bound to the APP peptide has been solved (17), but it is unknown how C-terminal sequences can inhibit APP binding. To elucidate the structural basis for the autoinhibition, we used X-ray crystallography. Under several conditions, the $Mint1^{453–643}$ fragment did not yield high-quality crystals. Because crystallization might have been hindered by two long loops that were not observable in the crystal structure of the PTB domain/APP-peptide complex and are thus likely to be flexible, we prepared Mint1 fragments with deletions of some residues from these loops (residues 499–508 and 569–

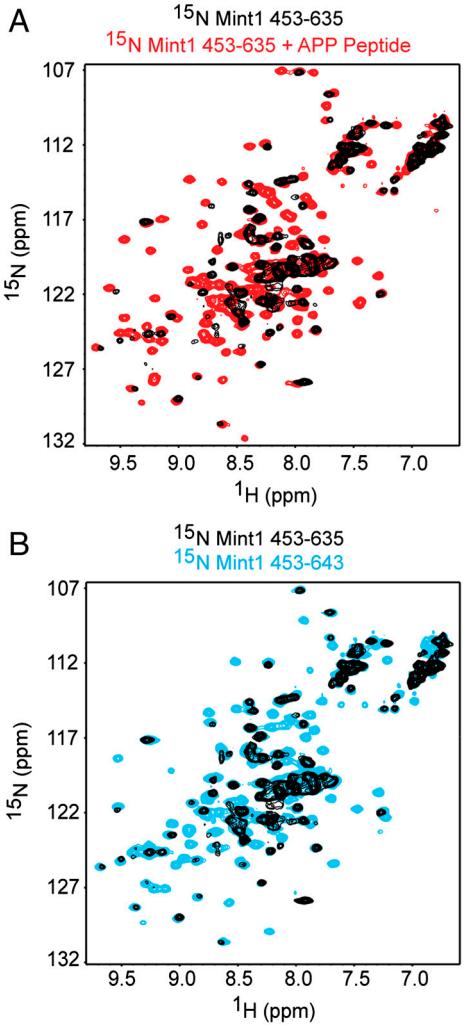

Fig. 2. Analysis of autoinhibition of the Mint1 PTB domain by NMR. (*A*) Superposition of ^{1}H-^{15}N HSQC spectra of ^{15}N-labeled Mint1 PTB domain (residues 453–635) in the absence (black contours) and presence (red contours) of the 15-residue APP C-terminal peptide. (*B*) Superposition of ^{1}H-^{15}N HSQC spectra of ^{15}N labeled Mint1 PTB domain (residues 453–635; black contours) and ^{15}N labeled Mint1 PTB domain with linker sequences (residues 453–643; blue contours) in the absence of APP peptide.

585). ITC showed that the Mint1$^{453–635}$ fragment containing the PTB domain with these loop deletions (Mint1$^{453–635*}$) binds to the APP C-terminal peptide with an affinity comparable to the intact PTB domain, and that C-terminal extension of this fragment by eight residues (Mint1$^{453–643*}$ fragment; referred here to as PTB*) inhibits APP-peptide binding (Fig. S5 *A* and *B*). Moreover, comparison of the ^{1}H-^{15}N HSQC spectra of Mint1$^{453–643}$ and Mint1$^{453–643*}$ showed that the overall structure of the domain is preserved after removing the loops (Fig. S6). Importantly, the Mint1 PTB* domain fragment yielded high-quality crystals that diffracted to a d_{min} of 1.9 Å. The crystal structure of the PTB* domain was solved by the single-wavelength sulfur anomalous dispersion method. The data collection and refinement statistics are described in Table S1.

A ribbon diagram of the PTB* domain (Fig. 3*A*) illustrates a canonical PTB structure with a common folding pattern known as the pleckstrin-homology (PH) domain superfold (18). The PH fold consists of a β-sandwich structure that contains seven antiparallel β-strands forming two orthogonal β-sheets, and is capped by a C-terminal helix (denoted as α2). Although most PTB domains that have been solved share low levels of sequence identity, structure-based alignments reveal that the core topological structure is evolutionary conserved (19). Like the PTB domains of Shc, disabled, and numb, the Mint1 PTB domain contains an N-terminal helix (α1) inserted between strands β1 and β2 (17, 20–22). Interestingly, our structure shows that the linker region C-terminal to the PTB domain forms a short helix (α3) that folds back onto the core structure of the PTB* domain and sterically hinders the APP binding site (Fig. 3*A*). Thus, the APP peptide binds at a groove formed by strand β5 and helix α2 of the Mint1 PTB domain (Fig. 3*B*), a binding mode that is shared among PTB do-

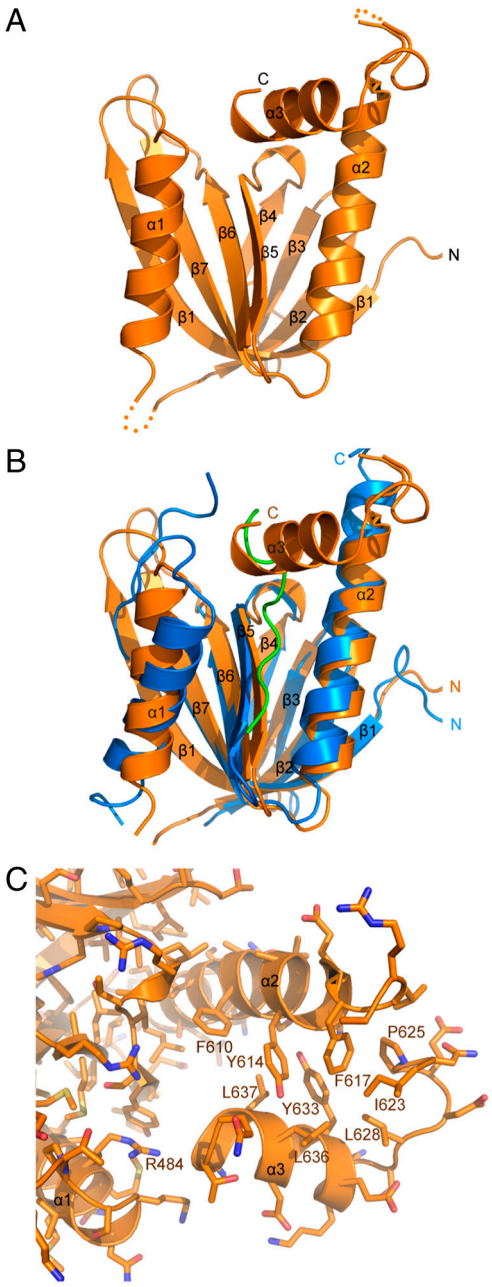

Fig. 3. Crystal structure of the autoinhibited Mint1 PTB* domain. (*A*) Ribbon representation of the Mint1 PTB* domain including C-terminal linker sequences (residues 453–643). The β-strands are labeled β1–β7, and the α-helices are labeled α1–α3. (*B*) Superposition of the Mint1 PTB* domain including C-terminal linker sequences (in orange) and the human Mint1 PTB domain (residues 453–633, in blue) complexed with the APP peptide (in green; ref. 17), illustrating how the autoinhibitory helix (α3) occludes the APP binding site. (*C*) Ribbon and stick diagram showing how the autoinhibitory helix packs against the core PTB domain. Carbon atoms are in orange, nitrogen atoms in blue, and oxygen atoms in red. Selected residues are labeled.

mains (17, 19). However, in the Mint1 PTB* domain structure, the helix α3 formed by the C-terminal extension (termed the "autoinhibitory helix") packs against strand β2 and helices α1 and α2, thereby blocking the center of the APP binding site. The intramolecular binding involves extensive hydrophobic interactions, particularly between the Tyr633, Leu636, and Leu637 side chains of the autoinhibitory helix and the Phe610, Tyr614, and Phe617 side chains of helix α2 (Fig. 3*C*). Additional hydrophobic contacts are formed by residues Ile623, Pro625, and Leu628. Moreover, the Arg484 side chain forms a hydrogen bond with the backbone of Asn638, and the Tyr614 side chain forms a hydrogen bond with the backbone of Leu636. Overall, our structure suggests that Mint1 normally adopts a closed conformational state where APP binding is blocked, and needs to undergo a transition to an open state in order to bind to APP.

Tyr633 is Key for Mint1 Autoinhibition. The Tyr633 side chain appears to play a central role in the intramolecular binding of the autoinhibitory helix in the structure of the Mint1 PTB* domain. To assess the importance of this residue for autoinhibition, we generated point mutations predicted to destabilize the hydrophobic interface and examined their effects on APP binding. We first determined whether the substitution of alanine for Tyr633, which was predicted to stabilize the helix but reduce the contribution of hydrophobic interactions with the PTB domain, affects APP binding. We produced a series of recombinant T7-tagged Mint1 fusion proteins harboring the Tyr633Ala (Y633A) mutation and used them in pull-down experiments to assay for their ability to bind endogenous APP from rat brain lysate or overexpressed APP, APLP1, or APLP2 from HEK293T cells (Fig. 4 *A* and *B*). The Y633A mutation released the autoinhibited conformation of the Mint1 PTB domain and substantially increased APP binding when the PTB domain is extended to include additional C-terminal residues. Similar effects of the Y633A mutation were also observed in the presence of the N-terminal or the longer C-terminal sequences of Mint1. Moreover, the Y633A mutation in full-length Mint1$^{1–839}$ increased APP-Mint1 binding compared to wild-type Mint1 without compromising the protein stability as evidenced by the similar levels of protein expression (Fig. 4 *A* and *B*, and Fig. S7). We further examined the binding affinity of the Mint1 Y633A mutant with the APP C-terminal peptide by ITC. Titrations showed that the Mint1 Y633A mutant restores the binding affinity of Mint1 for the APP C-terminal peptide (K_d = 1.7 μM) similar to that of the isolated PTB domain with the two loops deleted (Fig. S5*C*).

A Tyr residue analogue to Mint1 Tyr633 is conserved in Mint2, indicating that autoinhibition is likely a common feature and suggesting that the interaction of neuronal Mints with APP could be regulated by tyrosine phosphorylation. We therefore produced a Mint1 C-terminal protein (Mint1$^{453–839}$) that mimics a constitutively phosphorylated state by mutating Tyr633 to glutamic acid. As a control, we also made a conservative change in Tyr633 to phenylalanaine. We then assessed their ability to interact with APP, APLP1, and APLP2 in pull-down assays. We found the phosphomimetic Tyr633Glu (Y633E) mutation released the autoinhibition by C-terminal sequences on the PTB domain and enhanced Mint1 binding to APP, APLP1, and APLP2 from rat brain lysates, as well as binding of Mint1 to overexpressed APP from HEK293T cells (Fig. 4*C* and Fig. S8). In contrast, the Tyr633Phe (Y633F) mutant bound APP similar to the wild-type Mint1 C-terminal fragment. These results confirm that the hydrophobic contacts between the PTB domain and the autoinhibitory helix play a critical role in controlling the "tightness" of Mint1 autoinhibition, and suggest tyrosine phosphorylation as a potential mechanism for regulating the conformational change between states with low and high affinity for APP binding.

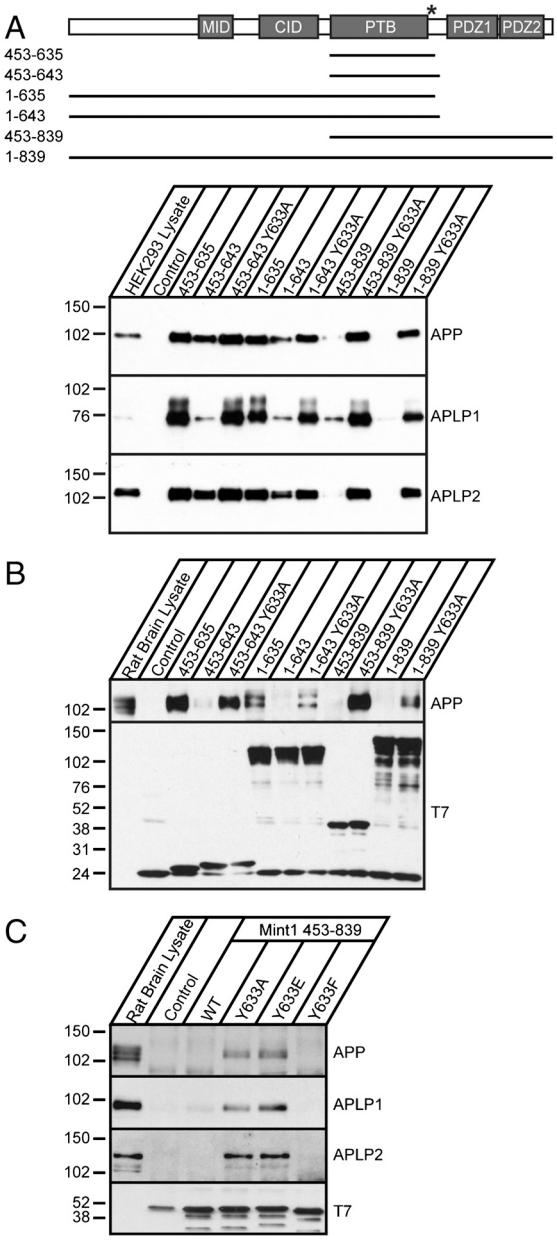

Fig. 4. Mutational analysis of Mint1 autoinhibition. (*A*) Illustration of Mint1 constructs used for binding with corresponding residues indicated on the left. The asterisk represents the Tyr633Ala (Y633A) point mutation. CID, CASK interacting domain. Western blot analysis of APP and APLPs bound to the different Mint1 recombinant proteins overexpressed in HEK293T cells and (*B*) of bound APP from rat brain lysate. Western blot analysis of the T7-tagged Mint1 proteins used for binding is shown below. (*C*) Mint1 C-terminal fusion proteins (residues 453–839) with Tyr633 substitutions to alanine (Y633A), glutamic acid (Y633E), or phenylalanaine (Y633F) were incubated with rat brain lysate and bound protein probed for APP and APLPs. Below is the Western blot analysis for T7-tagged Mint1 proteins.

Functional Role of Mint1 Autoinhibition in APP Processing. To examine the functional role of the two conformational states of Mint1 in APP processing, we cultured primary cortical neurons from an established mouse line with conditional alleles for all three Mint proteins (Mint triple floxed; MTF) harboring a transgene (tg) for coexpression of mutant APP and presenilin1 proteins (MTF^{tg}; ref. 15). Cultured MTF^{tg} neurons infected with an inactive *cre* virus show normal expression of all three Mints, whereas neurons infected with the active *cre* recombinase virus exhibit efficient deletion of all Mints (15, 23) (Fig. 5*B*). We have previously shown

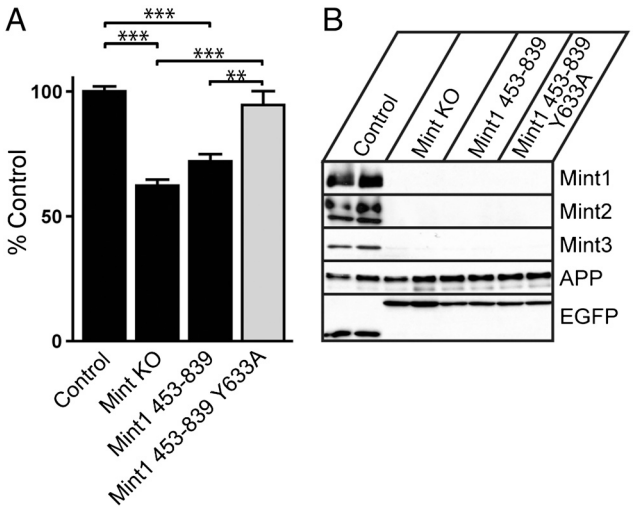

Fig. 5. Functional role of Mint1 autoinhibition in APP processing. Neurons were cultured from Mint triple-floxed newborn pups carrying one allele of a double transgene for mutant APP and presenilin-1, and infected with either lentivirus for inactive (control) or active *cre* recombinase (Mint KO), *cre*-IRES-Mint1$^{453–839}$, *cre*-IRES-Mint1$^{453–839\ Y633A}$. (*A*) Conditioned medium from Mint KO neurons expressing *cre* showed a significant decrease in Aβ42 levels compared to controls. A significant increase in Aβ42 levels was observed in Mint KO neurons expressing the Mint1$^{453–839\ Y633A}$ mutant as compared to Mint KO and Mint1$^{453–839}$ treated neurons. (*B*) Western blot analysis of Mint1, Mint2, Mint3, EGFP (*cre*), and APP protein levels in infected neurons. Data were normalized to control Aβ42 levels and expressed as mean ± SEM; ** $P < 0.01$, *** $P < 0.001$.

that cultured MTF^{tg} neurons infected with active *cre* recombinase have significantly lower levels of secreted Aβ40 and Aβ42, strongly supporting a role for Mint proteins in APP processing (15). We have used a lentivirus vector that contains an internal ribosome entry site (IRES) downstream of the *cre* or inactive *cre* coding region, and inserted coding sequences for truncated Mint1 proteins downstream of the IRES. This design allowed us to directly examine the effects of Mint1 mutants in the open and closed conformational states on APP processing in neurons lacking all endogenous Mints.

We compared the loss of Mint expression to control and IRES-dependent expression of the Mint1 C terminus (Mint1$^{453–839}$) with and without the Y633A mutation (Fig. S9). Mint knockout neurons exhibited significantly decreased production of Aβ42 compared to control neurons. Expression of the Mint1$^{453–839}$, where PTB-mediated binding to APP is impaired, led to a similar decrease in Aβ42 production as that observed in the Mint knockout neurons (Fig. 5*A*). Importantly, we found that the presence of the Y633A mutation within Mint1$^{453–839}$, which releases the autoinhibition of the Mint1 PTB domain, significantly increased Aβ production. These results suggest that the open conformation of Mint1 plays an important role in regulating APP processing, most likely through enhanced APP binding.

Discussion

It is well established that Mint1 binds APP and influences its proteolytic processing (3, 6, 16). However, little is known about the mechanisms that regulate APP binding to Mint1. The present study provides critical insights into this area by showing that sequences C-terminal to the Mint1 PTB domain inhibit APP binding through intramolecular interactions with the PTB domain (Figs. 1 and 2). The crystal structure reveals that C-terminal Mint1 sequences form an α-helix that folds back onto the PTB domain, resulting in an autoinhibited closed conformation of Mint1 that impedes APP binding (Fig. 3). Our results also show that the hydrophobic contacts between the PTB domain and the C-terminal inhibitory helix have a crucial role in stabilizing this closed conformation. Mutation of Tyr633 to Ala or Glu in the Mint1 autoinhibitory helix disrupted the autoinhibition, thereby facilitating APP binding and subsequent processing (Figs. 4 and 5). Overall, our data suggest that Mint1 must undergo a conformational switch from an autoinhibited closed state to an open state in order to bind APP, and that this switch plays an important role in regulating APP processing. It is tempting to speculate that this conformational switch could provide a potential point of intervention for therapies to treat AD.

Functional regulation by intramolecular interactions and conformational reorganization is likely a general property of adaptors and scaffolds, with Mint1 being a good example (24). Previous NMR studies observed intramolecular contacts between the Mint1 C-terminal tail and the PDZ1 domain, which blocks its ability to bind exogenous targets (25). Phosphorylation of a Tyr residue at the penultimate position in the C-terminal tail was proposed to disrupt its association with the PDZ1 domain, thereby liberating the PDZ1 domain to engage other ligands (25). Our data now show a different type of intramolecular inhibition within Mint1 whereby the region C-terminally adjacent to the Mint1 PTB domain forms an α-helix that occludes the APP binding site. This finding provides a rationale for the low levels of APP binding that are commonly observed with the full-length Mint1 protein. Altogether, the picture emerging from these observations suggests that an intricate network of autoregulatory interactions exists within Mint1. These interactions are likely critical for the mechanisms underlying how this multidomain adaptor protein facilitates and controls diverse neuronal signaling processes. Our study provides a first glimpse at atomic resolution of how the activity of the Mint1 PTB domain is controlled by an adjacent C-terminal sequence.

Mints 1–3 have isoform specific N-terminal regions and share highly conserved C-terminal sequences that consist of the PTB domain and two PDZ domains. Mint1 and Mint2 exhibit a high degree of conservation in the autoinhibitory sequences and are expressed in a neuron-specific manner. Not surprisingly, we found that the linker sequences at the C terminus of the Mint2 PTB domain also reduced APP binding (Fig. 1*C* and Fig. S3). This result suggests that Mint2 also possesses a conformational switch to regulate APP binding. Additionally, our results indicate that the autoinhibition of Mint1 and Mint2 regulates their interactions with the members of the APP family, all of which contain the conserved YENPTY cytoplasmic motif. As compared to Mints 1 and 2, the Mint3 PTB-PDZ1 linker sequence is most divergent around the autoinhibitory sequence, and the Mint1 Tyr633 is not conserved in Mint3. We propose that autoinhibition of APP binding only occurs with Mints 1 and 2, which have brain-specific functions related to APP that are not shared by the ubiquitous Mint3.

The fact that Mint1 can assume a low-affinity closed state and a high-affinity open state for APP binding raises the question of whether the transition between these states influences APP processing. Using rescue experiments in Mint-deficient neurons, we found that the presence of the Y633A mutation within the Mint1$^{453–839}$ C terminus increased Aβ production, reversing the reduction of Aβ levels in Mint-deficient neurons. This finding strongly supports the physiological relevance of the autoinhibitory PTB domain-α3 helix interaction as an important mechanism for regulating APP binding and processing events.

A potential mechanism that may relieve Mint1 autoinhibition could involve phosphorylation of Tyr633 because this residue is predicted to be an excellent substrate for the Src family of nonreceptor tyrosine kinases (26, 27) and a phosphomimetic mutant of Tyr633 shows increased APP binding. Thus, phosphorylation of Tyr633 might provide a natural means to relieve the inhibition caused by helix α3. Moreover, because Mints are multidomain adaptor proteins that bind to several synaptic and Alzheimer's-related proteins, it is plausible that these interactions also influence APP binding by inducing conformational changes in the

Mint1 protein. Such interactions could include presenilin (a γ-secretase component) and the presynaptic protein Munc18, which in previous studies has been suggested to modulate the actions of Mint1 on APP processing in nonneuronal cell lines (28), or with another as yet unidentified protein(s).

Adaptor proteins have often been thought to play passive roles in cellular signaling by tethering proteins of a specific signaling pathway. However, it is clearly recognized that they play a dynamic role in controlling the flow of cellular information to finely tune cellular responses and prevent uncontrolled activation through allosteric control (29). The present study represents a step in gaining structural and physiological insight into the dynamic regulation of the Mint1 adaptor protein and its interaction with APP. Our results suggest the possibility of designing small molecules that mimic the autoinhibitory helix to reduce APP processing as potential treatments for AD.

Materials and Methods

Affinity Chromatography. Transiently transfected HEK293T cells were washed with ice-cold PBS and lysed in 10 mM Tris-HCl, pH 8.0, 0.15 M NaCl, 0.25% NaN_3, 1% Triton X-100 containing protease inhibitors, incubated for 10 min on ice, and centrifuged at 16,000 × *g* for 10 min at 4 °C. Cell lysates were supplemented with 0.1 M NaCl, 2 mM β-mercaptoethanol, and protease inhibitors for binding and 0.5 mg of lysate was incubated overnight at 4 °C with 3 μg of T7-tagged protein. For rat brain binding experiments, unstripped rat brains (PelFreez Biologicals) were homogenized in 20 mM Tris, pH 8.5, and 10 mM EDTA containing protease inhibitors. Debris was removed by centrifugation at 1,100 × *g* for 10 min at 4 °C. The supernatant was centrifuged at 200,000 × *g* for 50 min at 4 °C. The resulting pellet was resuspended in 10 mM Tris, pH 7.6, 0.15 M NaCl, 1% Triton X-100, 1% Nonidet P-40 substitute containing protease inhibitors and incubated 1 h at 4 °C. Extracts were centrifuged at 100,000 × *g* for 45 min at 4 °C. β-Mercaptoethanol was added to 2 mM, and 1.5 mg of rat brain lysate was incubated with 3 μg of T7-tagged protein. Samples were washed in their respective binding buffers, resuspended in sample buffer, and analyzed by SDS-PAGE and immunoblotting using standard procedures (30, 31).

Isothermal Titration Calorimetry. ITC experiments were performed using a VP-ITC system (GE Healthcare) in PBS at 25 °C with samples of 20 μM Mint protein in the sample cell and successive injections of 200 μM APP C-terminal peptide (GQNGYENPTYKFFEQ), and the heat change was recorded for each injection. All Mint proteins were dialyzed overnight at 4 °C in PBS, centrifuged, and degassed before all experiments and the APP peptide was dissolved in PBS. The data were fitted with a nonlinear least-square routine using a single-site binding model with Origin for ITC version 5.0 (GE Healthcare).

NMR Spectroscopy. ^{1}H-^{15}N. HSQC spectra were acquired on Varian INOVA600 (Varian) at 25 °C. The sample solvent was H_2O/D_2O 95:5 (vol/vol). Samples contained 60 μM Mint1 fragments alone or with 70 μM APP peptide that was dissolved in 20 mM phosphate pH 8.0, 0.15 M NaCl and 1 mM tris(2-carboxyethyl)phosphine (TCEP).

X-Ray Crystallography. Purified Mint1 fragment (residues 453–643), but lacking residues 499–508 and 569–585 in two loops (PTB* domain) was concentrated to 14.6 mg/mL in buffer containing 10 mM Hepes pH 7.5, 0.15 M NaCl, and 2 mM TCEP. Crystals grew at 20 °C using the sitting drop vapor diffusion method. The drops in a ratio of 1:1 (protein/well solution) were equilibrated against 0.2 M ammonium acetate, 0.1 M Hepes pH 7.5, and 25% (vol/vol) isopropanol. Crystals appeared 24 h after the crystallization drops were set up and grew to the final size of 120 × 120 × 80 μm after 5 d. Cryoprotection was performed by serially transferring the crystals to a final solution of 25% (vol/vol) glycerol, 25% (vol/vol) isopropanol, 0.1 M Hepes pH 7.5, 0.15 M NaCl, 0.2 M ammonium acetate, and increasing in 5% steps of glycerol. Crystals were flash-frozen in liquid nitrogen, exhibited the symmetry of space group $P4_12_12$ with unit cell parameters of $a = 64.7$ Å, $c = 115.0$ Å, and contained one molecule of PTB* domain per asymmetric unit. Data were indexed, integrated, and scaled using the HKL-3000 program suite (32).

ACKNOWLEDGMENTS. We thank members of the laboratory, Drs. Uwe Beffert and Thomas Gilmore for comments and suggestions. Also, we thank Dr. Thomas Südhof (Stanford University, Palo Alto, CA) for plasmids and antibodies. This work was supported by grants from the National Institutes of Health (K01 AG027311 to A.H. and NS40944 to J.R.), the Alzheimer's Association (IIRG-09-130591 to A.H.), and by an American Heart Association fellowship to Y.X.

1. Okamoto M, Südhof TC (1997) Mints, Munc18-interacting proteins in synaptic vesicle exocytosis. *J Biol Chem* 272:31459–31464.
2. Okamoto M, Südhof TC (1998) Mint 3: A ubiquitous mint isoform that does not bind to munc18-1 or -2. *Eur J Cell Biol* 77:161–165.
3. Borg JP, Ooi J, Levy E, Margolis B (1996) The phosphotyrosine interaction domains of X11 and FE65 bind to distinct sites on the YENPTY motif of amyloid precursor protein. *Mol Cell Biol* 16:6229–6241.
4. McLoughlin DM, Miller CC (1996) The intracellular cytoplasmic domain of the Alzheimer's disease amyloid precursor protein interacts with phosphotyrosine-binding domain proteins in the yeast two-hybrid system. *FEBS Lett* 397:197–200.
5. Tanahashi H, Tabira T (1999) X11L2, a new member of the X11 protein family, interacts with Alzheimer's beta-amyloid precursor protein. *Biochem Biophys Res Commun* 255:663–667.
6. Tomita S, et al. (1999) Interaction of a neuron-specific protein containing PDZ domains with Alzheimer's amyloid precursor protein. *J Biol Chem* 274:2243–2254.
7. Haass C, De Strooper B (1999) The presenilins in Alzheimer's disease-proteolysis holds the key. *Science* 286:916–919.
8. Selkoe DJ (2001) Alzheimer's disease: Genes, proteins, and therapy. *Physiol Rev* 81:741–766.
9. Hardy J, Selkoe DJ (2002) The amyloid hypothesis of Alzheimer's disease: Progress and problems on the road to therapeutics. *Science* 297:353–356.
10. Sisodia SS, St George-Hyslop PH (2002) gamma-Secretase, Notch, Abeta and Alzheimer's disease: Where do the presenilins fit in? *Nat Rev Neurosci* 3:281–290.
11. Glenner GG, Wong CW (1984) Alzheimer's disease: Initial report of the purification and characterization of a novel cerebrovascular amyloid protein. *Biochem Biophys Res Commun* 120:885–890.
12. De Strooper B, et al. (1998) Deficiency of presenilin-1 inhibits the normal cleavage of amyloid precursor protein. *Nature* 391:387–390.
13. Struhl G, Adachi A (2000) Requirements for presenilin-dependent cleavage of notch and other transmembrane proteins. *Mol Cell* 6:625–636.
14. Yu C, et al. (2001) Characterization of a presenilin-mediated amyloid precursor protein carboxyl-terminal fragment gamma. Evidence for distinct mechanisms involved in gamma-secretase processing of the APP and Notch1 transmembrane domains. *J Biol Chem* 276:43756–43760.
15. Ho A, Liu X, Südhof TC (2008) Deletion of Mint proteins decreases amyloid production in transgenic mouse models of Alzheimer's disease. *J Neurosci* 28:14392–14400.
16. Mueller HT, Borg JP, Margolis B, Turner RS (2000) Modulation of amyloid precursor protein metabolism by X11alpha/Mint-1. A deletion analysis of protein-protein interaction domains. *J Biol Chem* 275:39302–39306.
17. Zhang Z, et al. (1997) Sequence-specific recognition of the internalization motif of the Alzheimer's amyloid precursor protein by the X11 PTB domain. *EMBO J* 16:6141–6150.
18. Macias MJ, et al. (1994) Structure of the pleckstrin homology domain from beta-spectrin. *Nature* 369:675–677.
19. Uhlik MT, et al. (2005) Structural and evolutionary division of phosphotyrosine binding (PTB) domains. *J Mol Biol* 345:1–20.
20. Zhou MM, et al. (1995) Structure and ligand recognition of the phosphotyrosine binding domain of Shc. *Nature* 378:584–592.
21. Li SC, et al. (1998) Structure of a Numb PTB domain-peptide complex suggests a basis for diverse binding specificity. *Nat Struct Biol* 5:1075–1083.
22. Stolt PC, et al. (2003) Origins of peptide selectivity and phosphoinositide binding revealed by structures of disabled-1 PTB domain complexes. *Structure* 11:569–579.
23. Ho A, et al. (2006) Genetic analysis of Mint/X11 proteins: Essential presynaptic functions of a neuronal adaptor protein family. *J Neurosci* 26:13089–13101.
24. Feng W, Zhang M (2009) Organization and dynamics of PDZ-domain-related supramodules in the postsynaptic density. *Nat Rev Neurosci* 10:87–99.
25. Long JF, et al. (2005) Autoinhibition of X11/Mint scaffold proteins revealed by the closed conformation of the PDZ tandem. *Nat Struct Mol Biol* 12:722–728.
26. Blom N, Gammeltoft S, Brunak S (1999) Sequence and structure-based prediction of eukaryotic protein phosphorylation sites. *J Mol Biol* 294:1351–1362.
27. Obenauer JC, Cantley LC, Yaffe MB (2003) Scansite 2.0: Proteome-wide prediction of cell signaling interactions using short sequence motifs. *Nucleic Acids Res* 31:3635–3641.
28. Ho CS, et al. (2002) Synergistic effects of Munc18a and X11 proteins on amyloid precursor protein metabolism. *J Biol Chem* 277:27021–27028.
29. Good MC, Zalatan JG, Lim WA (2011) Scaffold proteins: Hubs for controlling the flow of cellular information. *Science* 332:680–686.
30. Laemmli UK (1970) Cleavage of structural proteins during the assembly of the head of bacteriophage T4. *Nature* 227:680–685.
31. Towbin H, Staehelin T, Gordon J (1979) Electrophoretic transfer of proteins from polyacrylamide gels to nitrocellulose sheets: Procedure and some applications. *Proc Natl Acad Sci USA* 76:4350–4354.
32. Minor W, Cymborowski M, Otwinowski Z, Chruszcz M (2006) HKL-3000: The integration of data reduction and structure solution—from diffraction images to an initial model in minutes. *Acta Crystallogr D Biol Crystallogr* 62:859–866.